Decay of a Diamond Shock Pattern

GIRARD A. SIMONS*
Avco Everett Research Laboratory, Everett, Mass.

A solution is presented for the decay of the shock waves emanating from an infinite row of evenly spaced disturbances, placed perpendicular to an otherwise uniform, supersonic, two-dimensional flow. Analytic results indicate that the strength of the disturbances, relative to the conditions at infinity, decay as $\tilde{d}/\tilde{x}$ where $\tilde{x}$ is the downstream coordinate and $\tilde{d}$ is the spacing of the disturbances. This result, which is independent of the initial strength of the disturbance θ is valid for $\tilde{x}/\tilde{d} \gg 1/\theta$. The present solution is generally applicable to symmetrically placed disturbances in two-dimensional nozzle and channel flows. A specific example of disturbances generated in the gas dynamic laser (GDL) is examined in detail.

1. Introduction

DIAMOND shock patterns occur in nature as a result of the reflection of waves from solid boundaries and/or the contact surface separating two gases. Shock reflections from solid boundaries occur in supersonic channel and duct flows whereas those from contact surfaces are commonly found in an underexpanded rocket exhaust. Since the nature of wave reflections from solid boundaries and contact surfaces is of opposite sign, the discussion here is restricted to problems with solid boundaries. In particular, the geometry being considered is that in which the solid boundaries are aligned parallel to a uniform two-dimensional flow and the disturbances are aligned perpendicular to that flow.

A specific application for the decay of shock waves in this geometry lies in the gas dynamic laser (GDL). The GDL utilizes the rapid expansion of a heated gas through a series of adjacent two-dimensional supersonic nozzles to achieve the vibrational nonequilibrium required for lasing. Details of the GDL are given by Gerry.[1] Finite exit angles of the nozzle blades generate a diamond shock pattern as illustrated in Fig. 1. Since medium inhomogeneity may distort the laser beam, it is necessary to determine the rate at which these disturbances decay.

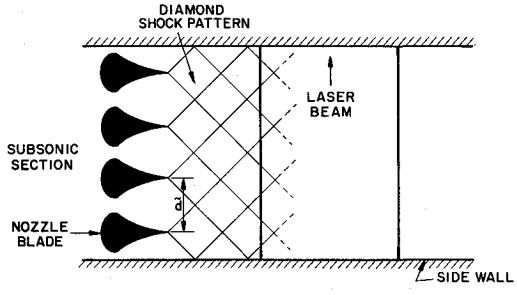

Fig. 1 GDL two-dimensional nozzle array.

Diamond shock patterns similar to that illustrated in Fig. 1 are also produced by other sources. The "sonic boom" from an infinite row of wings generates a wave pattern which, at infinity, is identical to that described above. This is illustrated in Fig. 2. Although the infinite geometry model is of little practical significance, it may be used to assess the decay of a disturbance in a two-dimensional channel flow. Symmetry at the walls of the channel imply that a disturbance placed in the center of the channel, or at the wall, will yield a wave pattern identical to that produced by an infinite row of evenly spaced disturbances. Hence, the asymptotic solution for the decay of the diamond shock pattern has application in several practical problems.

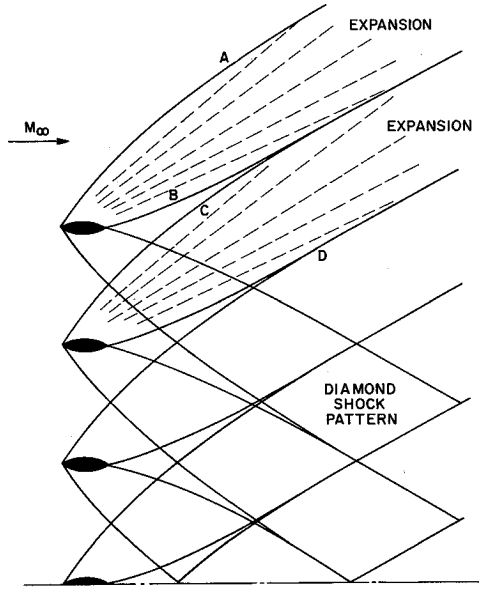

Fig. 2 Superposition of the sonic boom solutions.

A formalized method of applying acoustics to analyze disturbance propagation was set forth by Lighthill.[2] The acoustic solution for a single family of waves is rendered uniformly valid when written in characteristic coordinates with the location of the characteristics known to the accuracy of the solution on that characteristic. This general principle is often referred to as Lighthill's technique, or the method of strained coordinates, which describes its essential feature. Lighthill's technique was generalized to include two families of waves by Lin[3] who adopts characteristic parameters as the basis for a perturbation theory, which amounts to straining both families of waves.

Analysis of the propagation and decay of single disturbances has been reported by Landau,[4] Bethe,[5] Whitham,[6,7] and Lighthill.[8] These authors have considered the acoustic (far field) solution to the problems of the spherical blast wave and the sonic boom created by two-dimensional and axisymmetric bodies. They have applied Lighthill's technique to a single family of waves, corrected the location of the characteristics, and determined a consistent shock motion where waves of the same family intersected. In this way they were able to predict the rate at which the aforementioned disturbances decay.

Whitham[7] has applied this technique to analyze the flow past a wavy wall† (Fig. 3). He finds that the shocks decay as λ/y,

Received November 23, 1971; revision received March 30, 1972. This research was supported by the Air Force Weapons Laboratory, AFSC, United States Air Force, Kirtland Air Force Base, N. Mex. and Advanced Research Projects Agency, ARPA Order 870, under Contract F29601-69-C-0060.

Index categories: Lasers; Aerodynamic Noise.

* Principal Research Scientist. Member AIAA.

† See the Appendix of Whitham's paper.

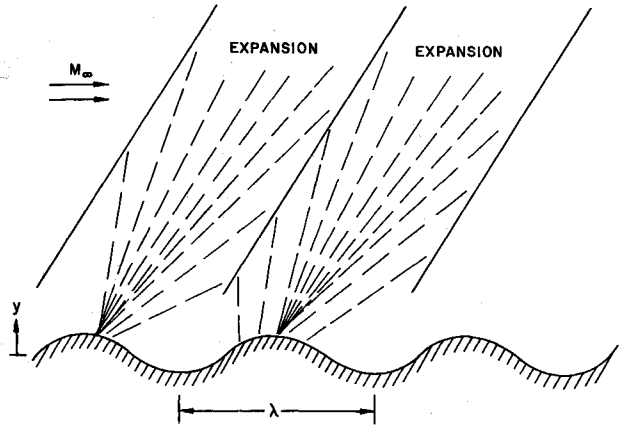

Fig. 3 Supersonic flow past a wavy wall.

where λ is the wavelength of the disturbance and y is the distance from the wall. Thus, the disturbance is independent of the height of the wall. Although not immediately obvious, this problem is very closely related to the decay of a diamond shock pattern. Whitham essentially considered an infinite row of evenly spaced disturbances aligned parallel with the flow. Thus, waves of only one family are generated. For disturbances aligned perpendicular to the flow, the coupling between the two families of waves must be included.

In the following sections, Lighthill's technique is used to analyze the decay of a diamond shock pattern. A general asymptotic solution is determined. It is shown that the coupling between the two families of waves is second order. Thus, Whitham's solution for the flow past a wavy wall is identical to that of the asymptotic decay of the diamond shock pattern. A uniformly valid solution for the decay of the GDL disturbance is generated and the region of applicability of the asymptotic solution is obtained.

2. General Formation

Following the general approach to small disturbance theory, we linearize about the free stream pressure, density and velocity. The solution of the two-dimensional acoustic equations is given by Shapiro[9]

$$P = -\gamma M_\infty^2 u; \quad \rho = -M_\infty^2 u; \quad u = \psi_1'(\eta) + \psi_2'(\xi)$$
$$v = \beta\psi_1'(\eta) - \beta\psi_2'(\xi); \quad \beta = (M_\infty^2 - 1)^{1/2} \tag{1}$$

where p, ρ, u, and v are the nondimensional perturbations of the pressure, density, axial velocity and transverse velocity. The variables ξ and η are constant along left and right running characteristics respectively and ψ_1 and ψ_2 are arbitrary functions of their respective arguments.

Within the framework of linear theory, ξ and η are constant along undisturbed Mach lines,

$$\xi = x - \beta y; \quad \eta = x + \beta y \tag{2}$$

where x and y are the axial and transverse coordinates and are nondimensionalized with respect to the disturbance spacing $\bar{d}$ (superscript $\sim$ implies a dimensional quantity).

Following Lin's extension of Lighthill's technique, Eq. (1) is a solution to the equations of motion in terms of ξ and η but Eq. (2) is not the correct location of the characteristics. A uniformly valid solution can be generated only by applying the first order solution on the first order characteristics, not the undisturbed characteristics. Thus, the problem is reduced to that of finding the corrections to Eq. (2).

From the general equations of the two-dimensional characteristics, we may express the slopes of the characteristics to first order in ψ_1' and ψ_2'.

The ξ characteristic

$$\left.\frac{dy}{dx}\right|_\xi = \frac{1}{\beta} + m_1\psi_2'(\xi) - m_2\psi_1'(\eta) + \Delta_\eta \tag{3}$$

$$m_1 = -(\gamma + 1)M_\infty^4/2\beta^3$$
$$m_2 = -M_\infty^2[(3 - \gamma)M_\infty^2 - 4]/2\beta^3$$

The η characteristic

$$\left.\frac{dy}{dx}\right|_\eta = \frac{-1}{\beta} - m_1\psi_1'(\eta) + m_2\psi_2'(\xi) + \Delta_\xi \tag{4}$$

where the discontinuity in the slope of a ξ characteristic in crossing an η shock† is designated by Δ_η and similarly for an η characteristic crossing an ξ shock by Δ_ξ.

Previous authors have considered problems with only one family of waves. That is, a single disturbance creating ξ or "outgoing" waves that attenuate the initial shock. In these cases, the last two terms on the right-hand side of (3) are dropped and Eq. (3) is easily integrated since ξ is constant on the characteristic. To describe an infinite row of disturbances perpendicular to the flow, we must consider the effects of both families of waves and shocks which, in general, complicates the integration of Eqs. (3) and (4).

When η characteristics intersect they form an η shock and the conservation laws require only that the shock bisect the angle between the characteristics.§ Dissipation within the shock then destroys the "information" that was carried by the characteristic and the isentropic flow observes only that the characteristic was "lost" in the shock. On the other hand, when ξ characteristics intersect an η shock, the conservation laws allow* the ξ characteristic to pass through with no change in the characteristic quantity $\psi_2'(\xi)$ but the ξ characteristic has a discontinuity in slope due to the difference in the gas dynamic properties on each side of the shock. This is illustrated in Fig. 4. The η^- characteristic is overtaken by the η shock whereas the η^+ characteristic overtakes the shock. The slope of the ξ characteristic below the η shock is given by (3), evaluated on the η^+ side of the shock.

$$\left.\frac{dy}{dx}\right|_\xi = \frac{1}{\beta} + m_1\psi_2'(\xi) - m_2\psi_1'(\eta_s^+)$$

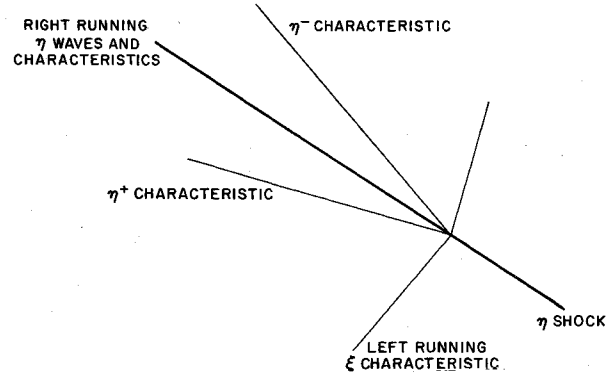

Fig. 4 Intersection of ξ and η characteristics at an η shock.

Similarly, above the shock, the slope of the characteristic is

$$dy/dx = 1/\beta + m_1\psi_2'(\xi) - m_2\psi_1'(\eta_s^-)$$

From these two expressions, we evaluate the change in the slope of the ξ characteristic in crossing an η shock

$$\Delta_\eta = m_2[\psi_1'(\eta_s^+) - \psi_1'(\eta_s^-)] \tag{5}$$

Similarly, for $\Delta\xi$ we obtain

$$\Delta_\xi = m_2[\psi_2'(\xi_s^+) - \psi_2'(\xi_s^-)] \tag{6}$$

where an ξ^+ characteristic is one which overtakes an ξ shock.

To first order, the ξ shock bends η characteristics and η shocks through the same angle. Similarly, the bending of ξ shocks and characteristics by the η shock is identical. Thus, Eqs. (5) and (6)

† An η shock is one that is formed by the coalescence of η characteristics.

§ If the shock is propagating into a uniform flow, one of the characteristics is an undisturbed Mach line.

* Here we are considering only the first-order terms when $\psi_1' = O(\psi_2')$.

represents the bending of both shocks and characteristics by shocks of the opposite family.

For later convenience, we split the motion of the shock into four parts

$$dy_{s_\xi}/dx = 1/\beta + d\delta_\xi/dx + dy_\eta/dx + \Delta_\eta \tag{7}$$

where y_{s_ξ} is the y coordinate of the ξ shock, δ_ξ is the contribution of the ξ characteristics, y_η is the effect of the η characteristics and Δ_η is the discontinuity in slope across and η shock.

A similar expression for the η shock is expressed in the same notation

$$dy_{s_\eta}/dx = -1/\beta + d\delta_\eta/dx + dy_\xi/dx + \Delta_\xi \tag{8}$$

Equations (3–8) must be solved for the location of the shocks and characteristics for arbitrary initial conditions, $\psi_1'(\eta)$ and $\psi_2'(\xi)$. Equation (1) may then be used to determine the flow perturbations everywhere in the physical plane. In the next section, this procedure is used to analyze the acoustic propagation from an infinite row of two-dimensional disturbances.

3. General Asymptotic Solution

The general problem to be considered is illustrated in Fig. 5. Assume an infinite row of disturbances, each represented by two intersecting shocks spaced distance $\tilde{d}$ apart.** The region over which the disturbance exists is $a\tilde{d}$. ψ_1' and ψ_2' are specified within this region and are identically zero elsewhere in the flowfield.

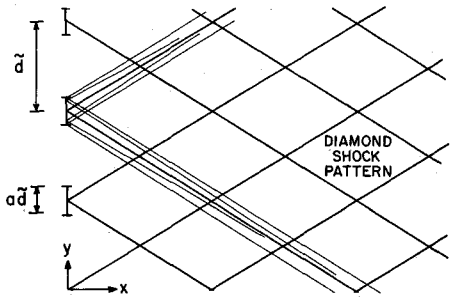

Fig. 5 Propagation from arbitrary two-dimensional disturbances.

Integration of the governing equations is simplified by the symmetric nature of the flow. A brief review of the sonic boom from a single disturbance is necessary to demonstrate this property.

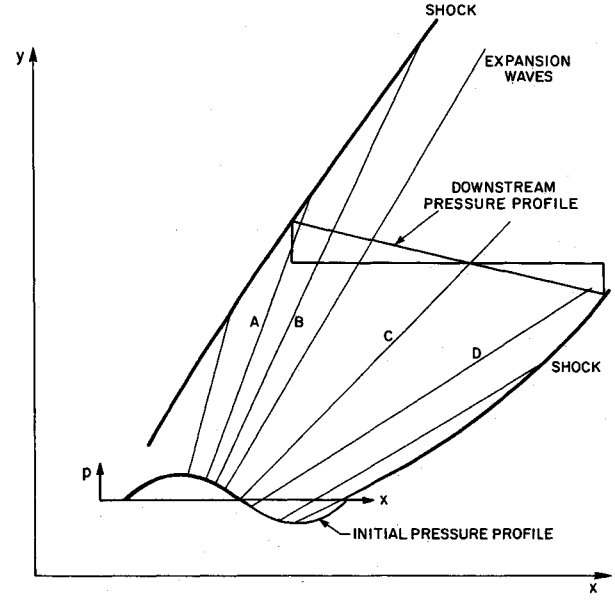

Fig. 6 Sonic boom solution.

** Spacing is unity in the nondimensional system.

The pressure profile created by some arbitrary disturbance is illustrated in Fig. 6. Waves A, B, C, and D, in the physical plane (x, y), propagate outward carrying information about the initial pressure profile. Linear theory predicts that each wave retains its initial value of the flow perturbations. Since the velocity of the wave depends upon the initial pressure, wave A will propagate faster than B and wave C will propagate as an undisturbed Mach wave. The waves moving faster than C attenuate the front shock and those moving slower attenuate the recompression shock.

When wave A intersects the shock, the value of the disturbance on that wave is dissipated within the shock. The isentropic flow is unaware of the viscous dissipation and observes only that the wave has been lost in the shock. This is the mechanism by which an isentropic solution predicts the decay of the disturbance. As $x \to \infty$, the pressure profile between the shocks is determined by the waves originating near $p = 0$. The pressure profile near $p = 0$ may be approximated by its tangent and it is this linear profile that is propagated downstream.

If we have a single disturbance in a supersonic flow, as illustrated by the top wing in Fig. 2, the sonic boom solution is valid. The first shock (A) propagates into the flow while the recompression shock (B) propagates downstream. The two shocks are weakened by an expansion centered between them and their strength decays to zero as the inverse square root of $\tilde{x}$ while the spacing between A and B increases as $(\tilde{x})^{1/2}$

If we place a second wing below the first, the same physical picture is consistent until shock waves B and C meet. Downstream of this point, there exists one shock attenuated from both sides by expansion waves. Extending these arguments to an infinite number of evenly spaced wings, we see that for every wing there exists one left running shock attenuated from each side by the centered expansion, and this left running shock pattern intersects an equivalent set of right running shocks and characteristics. This physical picture enables a gross simplification of the governing equations. Since the flow perturbations in the region between the shocks have a symmetric profile with corresponding positive and negative portions, it appears that a wave of the *opposite family* traversing the "boom" would feel no *integrated effect* of the boom. Here we treat this as an assumption to be verified a posteriori.

Suppose $\psi_1'(\eta)$ and $\psi_2'(\xi)$ are specified. Integration of (3) with the last two terms omitted illustrates that if $\psi_2'(\xi) < 0$, the ξ characteristics move faster than the undisturbed Mach wave and can catch the front shock. Similarly, when $\psi_2'(\xi) > 0$, the characteristics move slower than the undisturbed Mach waves and they are overtaken by the recompression shock. The situation is identical to that encountered in the sonic boom. As the bounding shocks move to infinity, it is the waves originating near $\psi_2'(\xi) = 0$ that cause the attenuation. Thus, we seek a solution, valid as x tends to infinity in which ψ_2' and ψ_1' tend to zero.

We integrate Eqs. (3) and (7) for the motion of the shock and characteristics, omitting, as previously stated, the integrated effect of the opposite family of waves

$$\begin{aligned} y|_{\xi^-} &= x/\beta + m_1\psi_2'(\xi^-)x + a/2 \\ y|_{\xi^+} &= x/\beta + m_1\psi_2'(\xi^+)x - a/2 \\ y_{s_\xi} &= x/\beta + \delta_\xi(x) \end{aligned} \tag{9}$$

where the constants of integration represent the y origin of the ξ characteristics in the limit of $\psi' \to 0$ $(x \to \infty)$. This is depicted in Fig. 7.

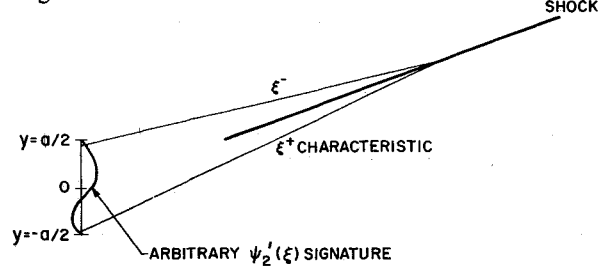

Fig. 7 Left running shock attenuated by expansion waves from the initial disturbance.

The characteristics and shock must intersect. Referring to ξ_s^+ as the value of ξ^+ at the intersection point x, and similarly for ξ_s^-, the requirements for the intersection become:

$$m_1 x[\psi_2'(\xi_s^+) - \psi_2'(\xi_s^-)] = a$$
$$\delta_\xi(x) = m_1\psi_2'(\xi_s^-)x + a/2$$

where $\psi_2'(\xi_s^+)$ and $\psi_2'(\xi_s^-)$ are functions of x since ξ_s represents the value of ξ hitting the shock at various locations.

At the point of intersection, the conservation laws require that the shock bisects the angle between the characteristics

$$d\delta_\xi/dx = m_1/2[\psi_2'(\xi_s^-) + \psi_2'(\xi_s^+)]$$
$$dy_\eta/dx = -m_2\psi_1'(\eta_s^+)$$

Solving the differential equations to determine δ_ξ, $\psi_2'(\xi_s^-)$ and $\psi_2'(\xi_s^+)$ is straightforward

$$\delta_\xi = 0; \quad \psi_2'(\xi_s^-) = -a/2m_1x; \quad \psi_2'(\xi_s^+) = a/2m_1x$$

Similarly, Eqs. (4) and (8) are solved for $\psi_1'(\eta_s^+)$ and $\psi_1'(\eta_s^-)$

$$\psi_1'(\eta_s^+) = -a/2m_1x; \quad \psi_1'(\eta_s^-) = a/2m_1x$$

In order to verify the assumptions imposed on the integrated effect of the waves of opposite family, we must determine the profiles of ψ_1' and ψ_2'. Since the waves at x originate within $0(1/x)$ of $\psi' = 0$, the shape of ψ' may be approximated by its tangent at $\psi' = 0$ and it is this linear profile that is propagated downstream. Hence, the lowest order terms in ψ' vary linearly between the shocks and the nonlinearities in the profile are second order in ψ' [here they are $0(1/x^2)$].

The integrated effect of the η waves on the motion of the ξ characteristic may now be determined. The last two terms on the right-hand side of Eq. (3) are illustrated in Fig. 8. The integrated effect of the $1/x$ terms are zero and the lowest order contributions of the second family to the locations of the first is the integral of the $1/x^2$ terms. Thus, the error in the location of the shock and characteristics, Eq. (9), is $0(1/x)$. This error also represents the terms that are second order in $\psi_2'(\xi)$.

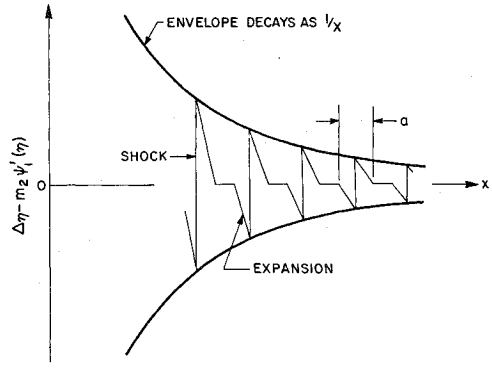

The density profile is given by the superposition of the ψ_1' and ψ_2' waves. Since the value of ψ' varies linearly across the expansion fan, superposition results in a density profile that is a plane in the (x, y, ρ) coordinates. For a completely disturbed flowfield, $(a = 1)$, the density fluctuations within the shock diamond vary linear with x from a maximum at the head of the diamond to a minimum at the rear of the diamond, as depicted in Fig. 9. For $a \neq 1$, the net density variation is obtained by superimposing the signatures illustrated in the bottom of Fig. 9. The maximum density disturbance, ρ_{max}, decays as $1/x$.

$$\rho_{max} = 2a\beta^3\bar{d}/(\gamma + 1)M_\infty^2\tilde{x} \qquad (10)$$

Equation (10) exhibits features that are extremely different from that of the decay of a single disturbance. Due to the attenuation of the shock by expansions on each side, the decay is much faster than the $1/(\tilde{x})^{1/2}$ result of the sonic boom. Perhaps the most striking result is that the disturbance is independent of its initial strength and now depends directly on the initial spacing of disturbances. The obvious difference between this problem and that of the sonic boom is that here the distance $\bar{d}$ controls the extent of the spreading of the disturbance whereas in the case of

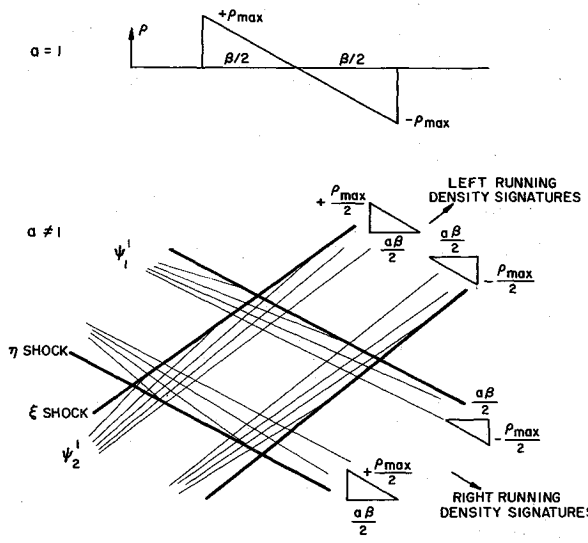

Fig. 9 Density profiles created by multiple disturbances.

the sonic boom, the disturbance itself is the regulating factor. Waves originating near $\psi' = 0$ that intersect the shock must travel in the $\tilde{y}$ direction a distance $a\bar{d}/2$ further than an undisturbed Mach wave. There is a unique strength associated with a wave that can traverse this additional distance in the time required to travel downstream to location $\tilde{x}$. Thus, the strength of the wave at $\tilde{x}$ is a direct function of $a\bar{d}$ and $\tilde{x}$. In the case of the sonic boom, doubling the initial disturbance (order θ) results in doubling the strength and spreading of the boom. However, at a fixed location within the boom, no change is felt. This is illustrated in Fig. 10.

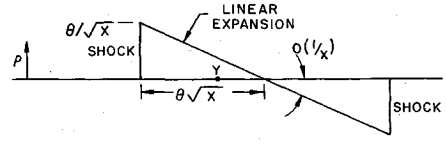

Fig. 10 The density profile in the far field sonic boom (N wave).

The width of the boom is $0[\theta(\tilde{x})^{1/2}]$, the gradient in the flow properties from the front to rear shock is $0(1/\tilde{x})$, independent of θ, and the peak disturbance is then $0[\theta/(\tilde{x})^{1/2}]$. Suppose we place an observer at point Y, distance $\bar{d}$ from the center of the boom. The observer will see a disturbance $0(\bar{d}/\tilde{x})$ for all $\tilde{x}$ independent of θ. This is the result given by Eq. (10). The extent of the boom is controlled by geometry rather than by θ. Thus, the disturbance becomes independent of θ and dependent only upon $\bar{d}$.

The result given in Eq. (10) is essentially identical to that of Whitham[7] for the flow past a wavy wall. However, two differences exist: First, the result has been extended to situations where both families of waves are present, and secondly, the results are now applicable to problems where only a fraction, "a," of the wavelength is disturbed.

It may be argued that Eq. (10) must possess knowledge of the initial disturbance through the generation of entropy. By virtue of the assumption that $\psi' \to 0$ as $x \to \infty$, the density fluctuations given by Eq. (10) are measured relative to the "freestream" conditions *at infinity*. No claim has been made that the downstream uniform state is independent of the disturbance. The integral form of the conservation laws must be used to determine the uniform state at infinity. Equation (10) then represents the rate at which this uniform state is approached.

4. Specific Applications

The geometry considered in the previous section has application to several multiple disturbance problems. In applying the results, the constant "a" must be evaluated after the shock waves have developed into the diamond pattern.

Figure 2 illustrates the sonic boom from an infinite row of wings. Shock waves B and C must intersect before the geometry of Fig. 5 is duplicated. This criterion can be expressed as

$$\tilde{x}/\tilde{d} > (\tilde{d}/\tilde{R})M_\infty$$

where $\tilde{R}$ is the size of the disturbance. The entire flow is now disturbed and the value of "a" is seen to be unity. For values of $\tilde{x}$ greater than $\tilde{d}^2M_\infty/\tilde{R}$, Eq. (10) applies and the disturbance is now independent of $\tilde{R}$ and dependent on $\tilde{d}$.

Disturbances placed in two-dimensional channel flows are also described by the general expression just derived. Horizontal planes of symmetry in Fig. 2 may be replaced by channel walls. Hence, solutions exist for disturbances placed in the center of the channel, on one wall, or those placed on both walls. Application of Eq. (10) requires only that the channel height be expressed in terms of $\tilde{d}$, the disturbance spacing.

The series of two-dimensional supersonic nozzles illustrated in Fig. 1 are designed to cancel all waves generated by the supersonic expansion. This requires that the nozzle blade be infinitely thin at the exit plane. The blades are truncated with some finite exit angle as depicted in Fig. 11. Shocks form at the exit plane to recompress the overexpanded flow. These shocks are attenuated from both sides by expansion waves and this problem falls into the general category of the multiple disturbance problem just considered.

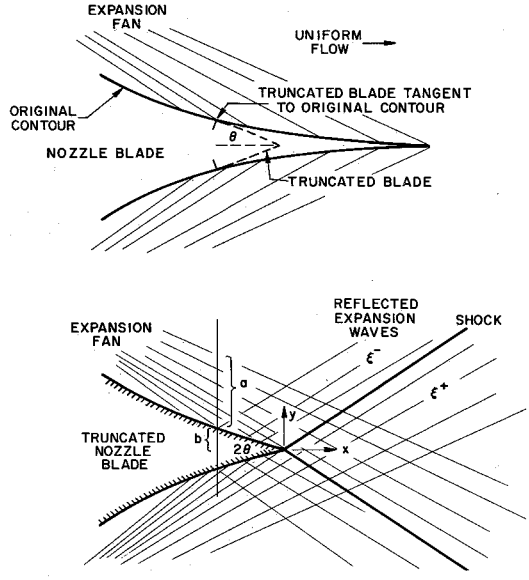

Fig. 11 Truncation of nozzle exit blade keeping the exit area unchanged.

The solution to this problem for all x will now be generated in order to indicate the values of x for which Eq. (10) is valid.

To model the disturbance generated at the nozzle exit plane, we assume that the flow near the wall has a transverse velocity that varies linearly from zero in the freestream to $-\theta$ at the wall. The details necessary to determine ψ' are given in Appendix A and only the results are quoted here. When $x = 0$,

$$\psi_2'(\xi^+) = (-\theta/a\beta)(y_0 + a/2); \qquad -a/2 \leqq y_0 < 0$$
$$\psi_2'(\xi^-) = (-\theta/a\beta)(y_0 - a/2); \qquad 0 < y_0 \leqq a/2$$

where the coordinate y is designated by y_0 to indicate that it is the origin of the ξ characteristic.

The formulation is identical to the previous case except now the origin of the characteristics are written as a function of $\psi_2'(\xi)$

$$y_0 = -a/2 - (a\beta/\theta)\psi_2'(\xi^+)$$
$$y_0 = a/2 - (a\beta/\theta)\psi_2'(\xi^-)$$

Integrating the equations of the characteristics and the shocks, applying the conditions of intersection and bisection, we determine the maximum density perturbation.

$$\rho_{\max} = \frac{M_\infty^2\theta}{\beta + \theta x(\gamma + 1)M_\infty^4/2a\beta^3} \tag{11}$$

The interpretation of Eq. (11) is straightforward. When $x = 0(1)$ and $\theta \to 0$, the expression returns to the equations of linear theory. However, when θ is fixed and $x \to \infty$ ($x \gg 1/\theta$), the nonlinear effects weaken the disturbance and it decays as given by Eq. (10). Although Eq. (11) is not as general as Eq. (10), it does demonstrate when the nonlinearities become dominant. Equation (10) applies to the GDL exit plane disturbance for $\tilde{x} \gg a\tilde{d}/\theta$.

Equation (10) is a general far field solution. However, the constant, a, must be carefully evaluated. We must allow the shocks from multiple disturbances to intersect, then evaluate "a" as the fraction of the flow field that is disturbed relative to the conditions at infinity. From this definition, it appears that "a" would always be unity since the conditions at infinity always differ from the upstream conditions by terms at least as large as $0(\theta^3)$, the entropy increase. However, for the nozzle exit disturbance, Eq. (10) does apply with $a \neq 1$ when $\rho > 0(\theta^3)$ but "a" must take on the value of unity when $\rho \leqq 0(\theta^3)$. This is discussed in Appendix A.

As a result of the analysis and examples cited previously, it appears that Eq. (10), with the proper choice of "a", may be applied quite generally as the far field solution for the decay of an infinite row of similar disturbances. As $x \to \infty$, "a" must always be unity. However, as illustrated in Appendix A, intermediate regions do exist where "a" depends upon the nature of the disturbance and is not necessarily equal to unity.

5. Discussion and Conclusions

Lighthill's technique has been applied to a general two-dimensional multiple disturbance problem and the propagation and decay of those disturbances have been determined. The strength of the disturbance in the far field has been shown to decay as $a\tilde{d}/\tilde{x}$, independent of the initial strength, and the location of the "far field" has been shown to be inversely proportional to the initial disturbance.

Proper representation of the far field requires knowledge of the constant "a" which represents the fraction of the flowfield that has been disturbed. For the sonic boom from an infinite row of wings, "a" is unity but for the nozzle exit disturbance depicted in Fig. 11, "a" may take on different values in different regions of the far field.

The results contained herein have been determined for two-dimensional flow. The propagation of a point disturbance inside a square supersonic duct would require a three-dimensional analogue to this work. By symmetry, the duct flow problem is equivalent to the sonic boom from an infinite plane of point disturbances where each disturbance lies on the corner of a square with the same dimensions as the duct. Although no such analysis has been carried out, one can again use the results of sonic boom to gain a feeling for the rate of decay. The sonic boom from an axisymmetric body spreads as $\theta x^{1/4}$ and decays as $\theta/x^{3/4}$ where θ represents the strength of the body. The signature within the boom is an N wave as illustrated in Fig. 10 for the two-dimensional case and the gradient is $0(1/x)$, independent of θ. Since geometry would again control the spacing of the shocks, the far field would see flow perturbations of order $\tilde{d}/\tilde{x}$, independent of θ. Further insight into this problem can be gained by imagining the shock pattern to be a series of cones with apex at the disturbance. The spacing between the cones is the disturbance spacing d. Far downstream, the radius of curvature of the shock, $\tilde{x}/\beta$, is much greater than d. Hence, the shocks appear to be planes and the problem appears to differ very little from that solved in the previous sections. Thus, multiple disturbances in both two and three dimensions appear to decay as $d/\tilde{x}$, although it has been proven only for the two-dimensional case.

Appendix A: Model for the Nozzle Exit Plane

In principle, a two-dimensional nozzle can be contoured such that the flow is brought to a uniform state as illustrated in Fig. 11.

However, this requires that the blade be infinitely thin at the exit plane. To avoid this difficulty, the nozzle blades are truncated at some finite angle as shown. A shock is then required to turn the flow at the nozzle exit.

At the point at which the truncated blade is tangent to the original contoured blade, we assume that the transverse velocity varies linearly from zero at the edge of the disturbed region to $-\theta$ at the wall. This information is carried by the right running waves and the function $\psi_1'(\eta)$ is determined.

$$\psi_1'(\eta) \doteq \theta\eta/a\beta^2 + K_0 \tag{A1}$$

where

$$\eta \doteq x + \beta y$$

and

$$K_0 \doteq [b - (a + b)\beta\theta]/a\beta^2$$

Continuity then constrains the integral of u over y at $x = -b/\theta$

$$\int_b^{a+b} u\,dy = -b/\beta^2 \tag{A2}$$

Conditions (A1) and (A2) then restrict "a" in terms of the blade geometry

$$a \doteq 2b/\beta\theta \qquad (\theta\beta \ll 1) \tag{A3}$$

Using (A3), K_0 can now be reduced to a simpler form

$$K_0 \doteq -b/a\beta^2$$

As the right running waves $[\psi_1'(\eta)]$ strike the truncated blade, the condition that $v = -\theta$ along the blade is satisfied by the generation of a left running family.

$$\psi_2'(\xi) \doteq \frac{\theta\xi}{a\beta^2} + \frac{\theta}{\beta} - \frac{b}{a\beta^2} \tag{A4}$$

where

$$\xi \doteq x - \beta y.$$

At the nozzle exit plane ($x = 0$), the functions ψ_1' and ψ_2' are given by

$$\begin{aligned} \psi_1'(\eta) &= (\theta/\beta)(y/a - \tfrac{1}{2}) + 0(\theta^2) \\ \psi_2'(\xi) &= (\theta/\beta)(\tfrac{1}{2} - y/a) + 0(\theta^2) \end{aligned} \tag{A5}$$

for $0 < y \leqq a/2$. These are the profiles that were used to model the exit plane disturbance.

The uniform conditions at infinity will differ from the original design conditions due to the generation of entropy. Since these terms are third order in θ, the exit plane model represents the flow perturbations with respect to the conditions at infinity to within the accuracy indicated in Eq.(A5). Thus, the disturbance, as seen by an observer at infinity, is $0(\theta)$ at the exit plane and decays in the manner prescribed by Eq. (11). When the disturbance decays in strength to $0(\theta^3)$, the far field sees a flow that is disturbed over its entire geometrical extent. This is illustrated in Fig. 12. The initial disturbance is referenced to the conditions at infinity and the point labeled "A" represents the downstream location at which the disturbance decays to $0(\theta^3)$. Beyond this point, "a" is unity since the entire flow is disturbed to the same order. Between "A" and "B," the shock propagates into an essentially uniform stream and decays as $1(x)^{1/2}$. Beyond point "B," Eq. (10) is again valid with "a" equal unity.

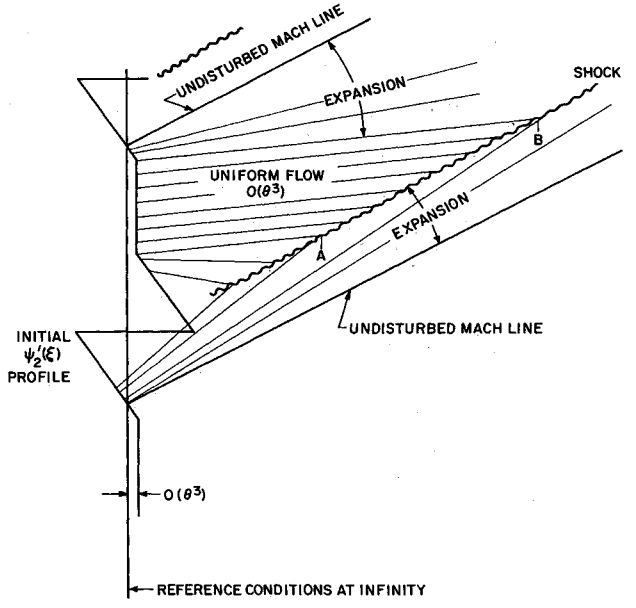

Fig. 12 Exit plane disturbance created by the nozzles illustrated in Fig. 11.

The strength of the density fluctuations are illustrated in Fig. 13. The transition of the decay rate from $a\tilde{d}/\tilde{x}$ to $\tilde{d}/\tilde{x}$ is seen to be the $1/(x)^{1/2}$ decay of the shock while passing through the uniformly disturbed region.

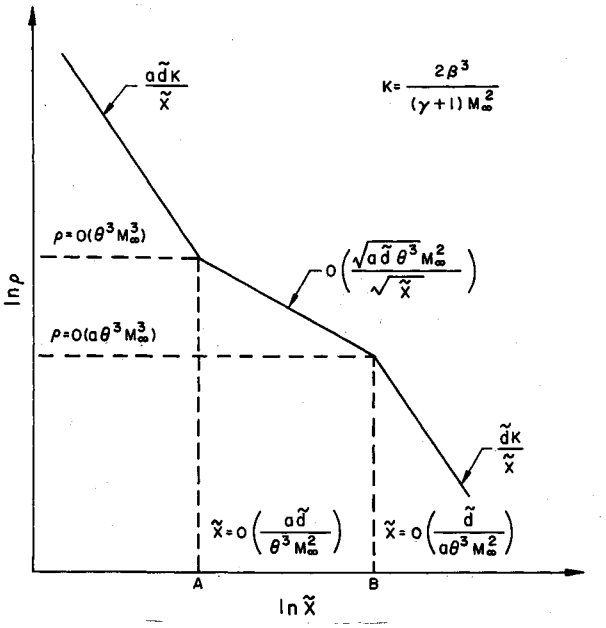

Fig. 13 Density fluctuations created by the exit plane disturbance.

The above arguments have been presented only to show consistency in the method and not to calculate the decay beyond the strength of the third-order terms. For this reason, the details of the transition in the decay near $\rho = 0(M_\infty^3\theta^3)$ have not been determined. It suffices only to say that such a transition does exist and as $x \to \infty$, the $\tilde{d}/\tilde{x}$ decay rate is recovered. Thus, for this nozzle exit plane model, the value of "a" can take on two values: "a_1" less than unity for $a_1\tilde{d}/\theta \ll \tilde{x} \ll a_1\tilde{d}/(\theta^3M_\infty^2)$ and "a_2" equal unity when $\tilde{x} \gg \tilde{d}/(a_1\theta^3M_\infty^2)$.

Appendix B: The Effect of Finite Nozzle Exit Angles on Laser Beam Distortion

With the decay of the strength of the diamond shock pattern illustrated in Fig. 1, there exists a relative phase shift between two light rays traversing the medium at different downstream locations. The phase shift of a single ray is given by Born and Wolf[10]

$$k\Psi = (2\pi\beta_0/\tilde{\lambda})\int \rho\,d\tilde{y}$$

Where $1 + \beta_0$ is the index of refraction evaluated at the freestream density and $\tilde{\lambda}$ is the wavelength of the electromagnetic wave.

The density profile in the flowfield is illustrated in Fig. 9. To lowest order, the density profiles are symmetric and the integral is zero. This is a consequence of the integral form of the continuity equation. It appears that we must determine the second-order terms in the solution to the disturbance propagation problem in order to determine the phase shift of an electromagnetic wave. However, we need only the integral of the density

perturbation, not the details of its profile. The integral may be evaluated from the integral form of the conservation laws, expressed in the perturbation variables.

Continuity: $\int (\rho + u + \rho u)\, dy = 0$

Momentum: $\int (p/\gamma M_\infty^2 + 2u + u^2 + \rho + 2\rho u)\, dy = 0(\theta^3)$

Entropy: $p = \gamma\rho + [\gamma(\gamma - 1)/2]\rho^2 + 0(\rho^3)$

Expanding these perturbations in an asymptotic series in θ,

$$\rho = \theta\rho_1 + \theta^2\rho_2 \cdots$$

where ρ_1, p_1, u_1, and v_1 obey (1), it is possible to determine the integral of ρ over y.

$$\int \rho_1\, dy = 0$$

$$\int \rho\, dy = \frac{[(\gamma - 1)/2]M_\infty^2 + 1}{M_\infty^2(M_\infty^2 - 1)} \int \theta^2\rho_1^2\, dy + 0(\theta^3)$$

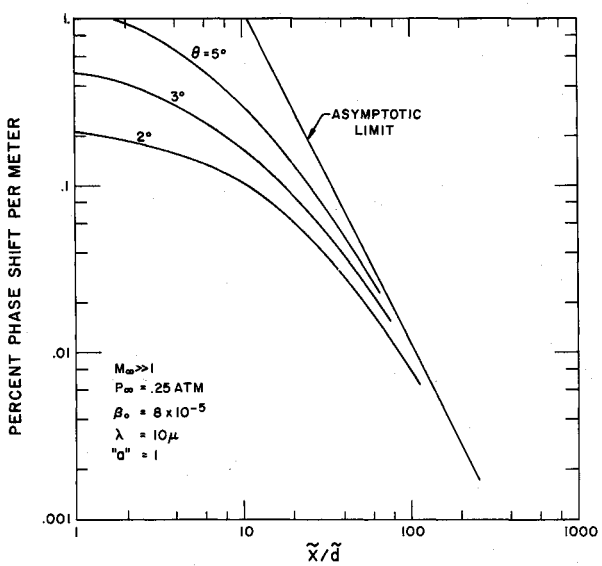

Fig. 14 Laser beam distortion.

For the case of the infinite row of two-dimensional disturbances, each such disturbance creates a left and right running set of waves. Carrying out the integration over these waves, we determine the pase shift of a single ray over the optical path $\tilde{L}$

$$k\Psi = \frac{\pi\beta_0\tilde{L}aM_\infty^2\theta^2\{[(\gamma - 1)/2]M_\infty^2 + 1\}}{3\tilde{\lambda}(M_\infty^2 - 1)^2(1 - m_1x\theta/a\beta)^2}$$

As $M_\infty \to \infty$:

$$k\Psi \to \frac{(\gamma - 1)\pi\beta_0\tilde{L}a\theta^2}{6\tilde{\lambda}(1 + (\gamma + 1)x\theta/2a)^2}$$

Figure 14 illustrates the percent phase shift per meter of a ten micron wave propagating through a flowfield with a free stream pressure of $\frac{1}{4}$ atmosphere ($\beta_0 \sim 8 \times 10^{-5}$) and $M_\infty \gg 1$. The relative phase shift across the beam may be determined by comparing the phase shift of the rays at the extremities of the beam.

References

[1] Gerry, E. T., "The Gas Dynamic Laser," *Laser Focus*, Dec. 1970, pp. 27–31

[2] Lighthill, M. J., "A Technique for Rendering Approximate Solutions to Physical Problems Uniformly Valid," *Philosophical Magazine*, Vol. 40, 1949, pp. 1179–1201.

[3] Lin, C. C., "On a Perturbation Theory Based on the Method of Characteristics," *Journal of Mathematics and Physics*, Vol. 33, 1954, pp. 117–134.

[4] Landau, L. D., "On Shock Waves Far from Their Source," *Prikladnaya Matematika i Mekhanika*, Vol. 9, No. 4, 1945, pp. 286–292.

[5] Bethe, H. A. et al., "Blast Wave," LA-2000, Aug. 1947, Los Alamos Scientific Lab., Los Alamos, N. Mex.

[6] Whitham, G. B., "The Behavior of Supersonic Flow Past a Body of Revolution Far from the Axis," *Proceedings Royal Society of London*, Ser. A, Vol. 201, March 1950, pp. 89–108.

[7] Whitham, G. B., "The Flow Pattern of a Supersonic Projectile," *Communications on Pure and Applied Mathematics*, Vol. 5, 1952, pp. 301–349.

8 Lighthill, M. J., "Higher Approximations in Aerodynamic Theory," *General Theory of High Speed Aerodynamics*, edited by W. R. Sears, Princeton University Press, Princeton, N. J., 1954, pp. 425–451.

[9] Shapiro, A. H., *The Dynamics and Thermodynamics of Compressible Fluid Flow*, Vol. I, Ronald Press, New York, 1953.

[10] Born, M. and Wolf, E., *Principles of Optics*, 3rd ed., Pergamon Press, New York, 1965.